Eur. J. Mineral.
2007, **19**, 783–789
Published online October 2007

Effect of incongruent dissolution on mineral solubility data derived from quench experiments

ANNE VERLAGUET* and FABRICE BRUNET

Laboratoire de Géologie, École Normale Supérieure, CNRS, 24 rue Lhomond, 75005 Paris, France
*Corresponding author, e-mail: verlaguet@geologie.ens.fr

Abstract: Weight-loss experiments in a double-capsule setup remain, to date, the most reliable source of mineral solubility data at HP and HT for geologically relevant systems. Recent experimental results (Verlaguet *et al.*, 2006: *Geochim. Cosmochim. Acta*, **70** (7), 1772-1788) obtained for the Al_2O_3-SiO_2-H_2O and K_2O-Al_2O_3-SiO_2-H_2O systems show that, in contradiction to what is generally assumed for quench experiments, incongruent dissolution products are likely to crystallize in the outer tube of the setup where most of the fluid is located. This result suggests that mineral solubility derived using the double-capsule setup are systematically overestimated. By modelling fluid reaction paths in simulated dissolution experiments (Al_2O_3-SiO_2-H_2O system), it appears that the overestimation of the aqueous species concentration in the high-pressure and high-temperature fluid can reach 50 to 100 % when pure water is used as starting fluid. The effect of changing the composition of the initial fluid on the derived solubility is discussed.

Key-words: weight-loss experiments, incongruent dissolution, fluid reaction path, mineral solubility, kyanite.

Introduction

Data on mineral solubility above 2–2.5 kbar (Walther & Orville, 1983; Woodland & Walther, 1987) are typically derived from quench experiments. Measurements after quenching (*e.g.*, weight loss) have been extensively used for determining the solubility of simple oxide minerals like quartz from 0.1 to 2 GPa at 400 to 900 °C (Anderson & Burnham, 1965, 1967; Pascal, 1984; Pascal & Anderson, 1989; Manning, 1994) and corundum from 50 MPa to 1 GPa at 400 to 800 °C (Anderson & Burnham, 1967; Pascal & Anderson, 1989; Azaroual *et al.*, 1996; Newton & Manning, 2003).

Data derived from quench experiments rely on measurements, mineral weight loss and/or fluid analysis (Gunter & Eugster, 1980), performed on a run product after it has been quenched to ambient conditions. Ideally, these experiments should be designed in such a way that the property which is measured to derive the solubility data is not affected by the late quench stage. In particular, the original fluid composition is barely preserved upon quenching. The solubility of minerals generally decreases with decreasing pressure and temperature. Therefore, during the quench event, changes in fluid composition are often accommodated by the formation of precipitates (quench products) and/or overgrowths around the solid phases of the experimental charge. This late crystallization stage appears as a major source of uncertainty on solubility data (*e.g.*, Manning, 1994).

An obvious way to overcome quench effects is to characterize aqueous fluids under high-pressure and high-temperature, *e.g.*, by *in-situ* synchrotron X-ray absorption (*e.g.*, Pokrovski *et al.*, 2002a, 2002b, 2003) or Raman spectroscopy (Zotov & Keppler, 2000, 2002). In particular, synchrotron X-ray fluorescence has been proven to yield accurate data on mineral solubility (*e.g.*, Schmidt & Rickers, 2003; Sanchez-Valle *et al.*, 2003, 2004). However, because of the attenuation of low-energy X-rays by the sample environment, synchrotron X-ray fluorescence is not suitable for the study of elements with low atomic numbers (*e.g.*, Si, Al, P) in diluted solutions, which limits its application to geologically relevant aqueous fluids. Therefore, there is still a considerable interest to use (and improve) measurements on quenched run products which should, eventually, be interpreted in light of *in-situ* spectroscopy results (*e.g.*, Zhang & Frantz, 2000; Newton & Manning, 2002, 2003).

With respect to quench experiments designed at characterizing the chemistry of aqueous fluids under pressure and temperature, a significant methodological improvement was achieved by Anderson & Burnham (1965) who developed a "tube-in-tube" setup which allows to separate quench products (external tube) from starting minerals (inner capsule). In this setup (Fig. 1), starting minerals are confined in an inner capsule which is perforated in order to allow only fluid and solute exchange with the external tube where most of the fluid phase is located. This setup (Fig. 1a, b) was first used in internally heated pressure vessels (Anderson & Burnham, 1965) and later adapted to piston cylinder experiments (Manning, 1994).

Recently, Verlaguet *et al.* (2006) used this type of experimental setup (Fig. 1a) to characterize mineral-fluid

DOI: 10.1127/0935-1221/2007/0019-1772
0935-1221/07/0019-1772 $ 3.15
© 2007 E. Schweizerbart'sche Verlagsbuchhandlung, D-70176 Stuttgart

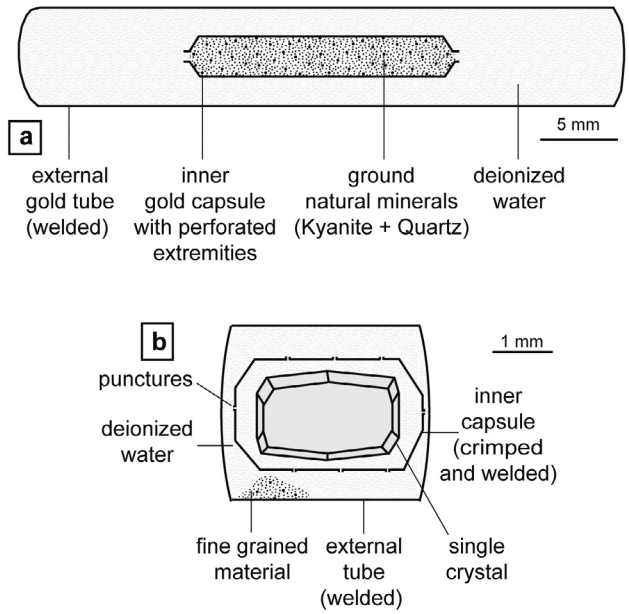

Fig. 1. Sketch of a tube-in-tube setup, designed for (a-) an internally-heated pressure vessel (setup used by Verlaguet *et al.,* 2006) and (b-) a piston-cylinder apparatus; the latter is derived from photos and setup description found in Newton & Manning (2003) and Manning (1994); the external tube has an arbitrarily length; very soluble material (*e.g.*, fine-grained) can be added to water in the external tube (Newton & Manning, 2002).

equilibration in the Al_2O_3-SiO_2-H_2O and K_2O-Al_2O_3-SiO_2-H_2O systems (ASH and KASH, respectively) for which incongruent dissolution is expected to occur (*e.g.*, Anderson & Burnham, 1983; Pokrovskii & Helgeson, 1991). They showed that incongruent dissolution is accompanied by the crystallization of secondary phases (unrelated to quench products) in the external tube. The crystallization of these secondary phases in the external tube of a tube-in-tube setup will invariably contribute to the weight loss of the material contained in the inner capsule. Similarly, any post-experiment analysis of both solid products collected in the external tube and fluid (Anderson & Burnham, 1983; Pascal, 1984; Anderson *et al.*, 1987; Pascal & Anderson, 1989; Manning & Boettcher, 1994) will include the contribution of these secondary phases. Consequently, if the results by Verlaguet *et al.* (2006) are generalized to solubility data derived using the tube-in-tube setup, it appears that the apparent mineral solubility measured by either the weight-loss technique or the quench-fluid analysis can be overestimated when incongruent dissolution leads to the crystallization of secondary phases in the external tube of the setup. This overestimate can be quantified if the amount of secondary phases crystallizing in the external tube is known.

On the basis of fluid reaction path modelling (Helgeson, 1968, 1979; Helgeson *et al.*, 1970), we will examine here how ignoring this type of secondary crystallizations or misinterpreting them as quench products can lead to overestimated solubility data.

Overestimation of solubility data derived from quench experiments, due to incongruent dissolution

Quantification of the amount of secondary phases related to incongruent dissolution

We will simulate here the derivation of the solubility of the assemblage kyanite + quartz in pure water (ASH system), for two different quartz/kyanite molar proportions (10/1 and 1/1) and two *P-T* conditions (0.5 GPa – 550 °C and 1.2 GPa – 800 °C). The amount of secondary phases produced by incongruent dissolution is calculated by modelling the fluid reaction path, *i.e.*, the evolution of the fluid composition during fluid-mineral equilibration.

The *basic equations* are the mass balance among mineral phases and aqueous species (1), the mass action law (2), and the electroneutrality (3):

$$\Delta m_i = \Sigma_{j=1}^{N} (n_j / W_{\mathrm{H_2O}}) \cdot \alpha_{i,j} \quad (1)$$

where Δm_i represents the change in the molality of the aqueous species containing chemical element i, during fluid-mineral equilibration, $\alpha_{i,j}$ the mole ratio of element i in mineral j/aqueous species, n_j the number of moles of dissolved (+) or crystallized (–) mineral j and W_{H_2O} the mass of water (kg).

$$K = \Pi a_i^{\alpha_i} \quad (2)$$

where K is the equilibrium constant of the incogruent dissolution reaction, a_i is the activity of each aqueous or solid species, and α_i is the stoichiometric coefficient of the aqueous or solid species i in the reaction.

$$\Sigma_{i=1}^{N} m_i \cdot \beta_i = 0 \quad (3)$$

where β_i is the charge of the aqueous species i.

The *assumptions* made to perform the calculation are:

1- The first stage of the fluid-mineral equilibration is controlled by the proportion and the respective dissolution kinetics of the two starting minerals. We will assume similar dissolution kinetics for both quartz and kyanite (see Verlaguet *et al.,* 2006 for the details on the relevant kinetic data); this implies that the starting minerals dissolve according to their respective molar proportions.

2 The real shape of the fluid reaction path depends on the relative kinetics of starting mineral dissolution *versus* secondary phase crystallization; here we will model a "partial equilibrium reaction path" for which a mineral precipitates at equilibrium when the fluid becomes saturated with respect to this phase. We also assume that the fluid composition is homogeneous in the setup (*i.e.*, all the fluid follows the same reaction path, whatever its location in the setup).

3 Following Verlaguet *et al.* (2006), it will be assumed that the dissolution reaction at 0.5 GPa – 550 °C produces two dominant aqueous species, $Al(OH)_4^-$ and $H_4SiO_4^0$, whose activity coefficients (γ) are considered to be 1. Water activity (aH_2O) is taken to be 1; both quartz and kyanite are pure endmembers, so their activities are also 1.

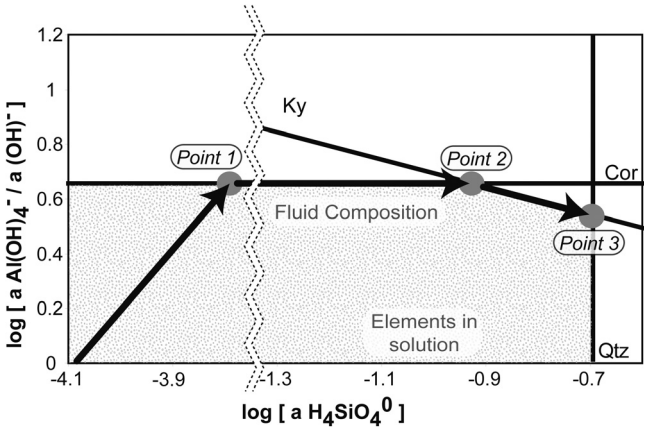

Fig. 2. Activity diagram, log ([a $Al(OH)_4^-$] / [a OH^-]) *vs.* log [a $H_4SiO_4^0$], representing the fluid saturation curves with respect to corundum (Cor), kyanite (Ky) and quartz (Qtz) at 550 °C – 0.5 GPa. The data for mineral solubility were computed with SUPCRT92 and its updated database (Shock *et al.,* 1997). These curves limit the field of fluid undersaturation with respect to all considered minerals (shaded area). The bold lines with black arrows underline the partial equilibrium reaction path of the fluid (initially pure water) while it equilibrates with the starting minerals quartz + kyanite introduced in molar proportions 10:1. Due to incongruent dissolution of the assemblage kyanite + quartz, the fluid will successively saturate with respect to corundum (Point 1) and kyanite (Point 2) before reaching its equilibrium concentration (Point 3); both solid phases are expected to crystallize.

The *solubility data* at 0.5 GPa – 550 °C are derived using the program SUPCRT92 (Johnson *et al.*, 1992) and its updated database (Shock *et al.*, 1997) to calculate equilibrium constants (log K) for fluid-mineral reactions. At 1.2 GPa – 800 °C, solubility data for corundum, corundum + kyanite and quartz were taken from experimental data by Newton & Manning (2003). The solubility of kyanite + quartz was also inferred from these data, considering that mineral dissolution releases one dominant aqueous species for each Al and Si, *i.e.*, ignoring any possible Al-Si complex. At 1.2 GPa – 800 °C, the amount of secondary phases could be quantified without determining the fluid speciation, because we used directly molality data.

Results – The modelled fluid reaction path is depicted on the activity-activity diagram (Fig. 2). The dissolution of the starting minerals in initially pure water is congruent as long as the fluid is undersaturated with respect to all mineral phases in the system (*i.e.*, on the path to Point 1, Fig. 2). In a fluid in equilibrium with quartz + kyanite at both 0.5 GPa – 550 °C and 1.2 GPa – 800 °C, the aqueous-Al molality is 2 to 4 orders of magnitude lower than the aqueous-Si molality. Thus the fluid composition will first reach saturation with respect to an Al-phase, namely corundum (Point 1, Fig. 2). At point 1, the fluid is still undersaturated with respect to both starting minerals, whose dissolution should continue. However, on the path between Point 1 and Point 3 (Fig. 2), the dissolution of kyanite + quartz proceeds incongruently, *i.e.*, corundum (secondary phase) must crystallize in order to store any Al released by further kyanite dissolution. Simultaneously, the concentration of aqueous-Si increases in the fluid. Accordingly, the fluid composition is expected to evolve along the corundum saturation curve until the fluid reaches saturation with respect to kyanite (path between Points 1 and 2, Fig. 2). At Point 2, however, the fluid is still undersaturated with respect to quartz. Secondary kyanite is expected to crystallize (path between Points 2 and 3, Fig. 2) while quartz from the starting mixture is still dissolving. The fluid reaction path is achieved when saturation with respect to the stable mineral assemblage (*i.e.*, kyanite + quartz) is attained (Point 3, Fig. 2).

Thus as a result of incongruent dissolution, corundum and kyanite should successively form in the system. However, in a ternary system as ASH, at the *PT* conditions of the experiments, no more than two solid phases can coexist with the fluid (*e.g.*, Point 2, Fig. 2). Therefore, under equilibrium conditions, the fluid composition cannot evolve (from Point 2 to 3, Fig. 2) unless the first solid phase (*i.e.*, corundum) has completely disappeared. Finally, only secondary kyanite should remain when the fluid has equilibrated with the initial minerals (Point 3, Fig. 2).

The number of moles of secondary kyanite (n^+_{Ky}) produced by incongruent dissolution is obviously proportional to the fluid volume (V_{fluid}). Therefore, amounts of secondary phases are expressed in Table 1 as volumetric percentages (*i.e.*, normalized to the total fluid volume, V_{fluid}). It can be seen in Fig. 2 that the molality of $H_4SiO_4^0$ at Point 1 depends on the proportion of Al and Si released by the starting solid-phases into the fluid. In the case of the equilibration of kyanite + quartz with pure water at 550 °C – 0.5 GPa, secondary phases represent 0.25 % and 0.05 % of the fluid volume for a starting quartz/kyanite proportion of 1/1 and 10/1, respectively. Similarly, at 800 °C – 1.2 GPa, the amount of secondary phases varies from 2.2 % to 0.4 % of the fluid volume when the quartz/kyanite proportion varies from 1/1 to 10/1, respectively (Table 1). For a similar quartz/kyanite ratio, secondary phases are calculated to be much more abundant at 800 °C – 1.2 GPa, because the difference between aqueous-Al and -Si molality in equilibrium with kyanite + quartz is higher (m_{Si} / $m_{Al} \approx 10^3$ to 10^4) than at 550 °C – 0.5 GPa (m_{Si} / $m_{Al} \approx 10^2$ to 10^3).

Solubility overestimation in the quartz-kyanite mineral system

Weight-loss technique – In a tube-in-tube setup, the effect of these secondary phases on solubility data will strongly depend on their location in the setup. Ideally, the measured weight loss (g) in the inner capsule (IC), ΔW_{IC}, can be expressed as follows, assuming that secondary kyanite crystallization occurs exclusively in the IC:

$$\Delta W_{IC} = n_{Qtz} \cdot M_{Qtz} + n_{Ky} \cdot M_{Ky} \quad (4)$$

where n_{Qtz} and n_{Ky} are the number of moles of quartz and kyanite respectively, either dissolved (+) or crystallized (–) during fluid-mineral equilibration. M_{Qtz} and M_{ky} are the molar masses of these two minerals (g/mole). Assuming that the initial fluid is free of both silica and alumina,

Table 1. Calculated amount of secondary phases and consecutive error on apparent solubility considering the incongruent dissolution of the assemblage kyanite + quartz in pure water.

P-T conditions	quartz : kyanite (molar ratio)	secondary phases (% of V_{fluid}) [a]	Fluid + quench m_{Al} overest. [b,d]	Fluid + quench m_{Si} overest. [b,d]	Weight-loss m_{Si} overest. [c,d]
550 °C – 0.5 GPa	10:1	0.05 %	× 600	5 %	15 %
550 °C – 0.5 GPa	1:1	0.25 %	× 3300	30 %	80 %
800 °C – 1.2 GPa	10:1	0.4 %	× 80	5 %	20 %
800 °C – 1.2 GPa	1:1	2.2 %	× 430	35 %	95 %

[a] Amount of secondary phases calculated for a partial equilibrium fluid reaction path, and expressed in percentage of the fluid volume. Data for mineral solubility computed from SUPCRT92 and its updated database (Shock *et al.*, 1997) at 550 °C – 0.5 GPa, and taken from Newton & Manning (2003) at 800 °C – 1.2 GPa.

[b] Overestimation of aqueous-Al (m_{Al}) and aqueous-Si (m_{Si}) molality derived from fluid plus quench product analysis.

[c] Overestimation of aqueous-Si molality (m_{Si}) derived by the weight-loss technique in a tube-in-tube setup.

[d] Maximum overestimation on the apparent molality (m_{Al} and m_{Si}), calculated considering that all the secondary phases crystallized in the external tube of the tube-in-tube setup.

Eqs. (1) and (4) can be combined to relate molality and weight loss:

$$\Delta W_{IC}/W_{H_2O} = m_{Si} \cdot M_{Qtz} + 1/2\, m_{Al} \cdot (M_{ky} - M_{Qtz}) \quad (5)$$

Since the concentration of aqueous-Al is negligible compared to that of aqueous-Si (m_{Si} / m_{Al} ≈ 10^2 to 10^4), Newton & Manning (2003) have stated that the weight-loss technique actually measures the silica concentration in the fluid. Therefore:

$$\Delta W_{IC}/W_{H_2O} \approx m_{Si} \cdot M_{SiO_2} \quad (6)$$

However, Eqs. (4) and (5) are valid only if all the secondary phases crystallized in the inner capsule, *i.e.*, if they are taken into account in the measured weight loss (ΔW_{IC}). If x percent of kyanite crystallized in the external tube, then the apparent Si molality (m_{Si}^{ap}) is:

$$m_{Si}^{ap} = m_{Si} + x \cdot n_{Ky}^{+}(M_{Ky}/M_{SiO_2})/W_{H_2O} \quad (7)$$

which is an overestimation of the true Si molality (m_{Si}); n_{Ky}^{+} is the total number of moles of secondary kyanite. In the worst case, *i.e.*, if all the secondary phases would crystallize in the external tube (*i.e.*, $x = 1$ in Eq. (7)), the use of the weight-loss technique will lead to an aqueous silica molality overestimate by 80 % for a 1/1 molar ratio and by 15 % for a 10/1 ratio (550 °C – 0.5 GPa). At 800 °C – 1.2 GPa, aqueous silica molality will be overestimated by 95 % for a 1/1 molar ratio and by 20 % for a 10/1 molar ratio (Table 1).

Fluid plus quench products analysis – The alternative technique, which involves analysing both the fluid and the external tube products, allows one to determine both silica and alumina contents of the fluid at high pressure and high temperature (HP-HT fluid). However, if secondary phases partly form in the external tube (x percent), the measured Si and Al molalities (m_{Si}^{ap} and m_{Al}^{ap} respectively) will correspond to overestimations of the true molalities:

$$m_{Si}^{ap} = m_{Si} + x \cdot n_{Ky}^{+}/W_{H_2O} \quad (8)$$

$$m_{Al}^{ap} = m_{Al} + x \cdot 2n_{Ky}^{+}/W_{H_2O} \quad (9)$$

Again, assuming the case where all secondary kyanite would be restricted to the external tube ($x = 1$), the silica content of the HP-HT fluid will be slightly overestimated (by 5 % for a 10/1 ratio and by 30–35 % for a 1/1 ratio) whereas the alumina content will be greatly overestimated (Table 1). At 550 °C – 0.5 GPa and 800 °C – 1.2 GPa respectively, the m_{Al} will be overestimated by 3300 and 430 times for a mineral ratio of 1/1, and by 600 and 80 times for a mineral ratio 10/1 (Table 1).

Discussion: how to improve solubility measurements?

Distribution of secondary phases between inner capsule and external tube

The weight-loss technique and the analysis of fluid plus quench products in a double-capsule setup remain undoubtedly the most reliable techniques to date for quantifying mineral solubility at high pressure and temperature. Unfortunately, the accuracy of these solubility data can be altered by secondary mineral crystallization when incongruent dissolution occurs, as in most naturally relevant systems. Furthermore, it is difficult to subtract the contribution of these secondary phases, especially because their exact distribution within the setup cannot be ascertained. For example, Verlaguet *et al.* (2006) showed that at 550 °C – 0.5 GPa, these secondary phases display characteristic morphologies and can therefore be easily distinguished from the amorphous-like quench products. However, at higher pressure and temperature or in systems involving more soluble species, the identification of secondary phases may be more difficult because the proportion of quench products is higher, and for phases with high surface-solution exchange rates (*e.g.*, calcite), their euhedral morphology can be achieved upon quenching. Indeed, as shown by Verlaguet *et al.* (2006), secondary phases in the external tube of a tube-in-tube setup may be partly or completely covered by quench products. Moreover, the exact distribution of secondary products between external

tube and inner capsule could not be determined by Verlaguet *et al.* (2006), because these phases could not be distinguished in the inner capsule due to the persistence of abundant starting minerals. However, the proportion of these secondary phases observed in the external tube was not even marginal because their volume, estimated by eye, was of the same order of magnitude as the total secondary phase volume retrieved from modelling of the fluid reaction path in these experiments. One could consider that the proportion of secondary phases between inner capsule and external tube would reflect their relative fluid volumes. Then, similarly to the quench products, secondary minerals would mainly occur in the external tube. However, in the particular case where secondary phases and starting minerals are the same, the latter may act as seeds in the inner capsule and will favour *in-situ* re-crystallization. Furthermore, accurate modelling of the fluid reaction path requires dissolution kinetic data as well as aqueous diffusion data at high pressure and high temperature, which are not available. It is therefore hazardous to correct solubility data for the contribution of secondary phase crystallization in the external tube: only a maximum error can be safely inferred, by considering the case where all the secondary phases are located in the external tube (Table 1).

Addition of silica in the starting fluid: a way to improve the accuracy of solubility data

One can try to minimize the effect of incongruent dissolution by changing the starting composition of the aqueous fluid. As shown in Fig. 2 for the ASH system, Al-bearing secondary phases crystallize as long as silica saturation is not achieved. As already mentioned, this is due to the relatively high solubility of aqueous silica, ASH being one of the chemical systems for which the solubility contrast between the two components (*i.e.*, between Al_2O_3 and SiO_2) is the more pronounced.

Figure 3 displays a series of fluid reaction paths, considering starting fluids with various silica contents. The composition of the starting fluid is expressed in percentage of the equilibrium molality of aqueous-Si ($m_{H_4SiO_4^0}$). Equilibrium with the mineral assemblage kyanite + corundum can be attained from an initial fluid which is undersaturated or supersaturated in silica with respect to kyanite + corundum (*i.e.*, containing respectively less than 100 % and more than 100 % of the equilibrium value of $m_{H_4SiO_4^0}$). It is important to note that in both cases, the initial fluid is undersaturated in aqueous-Al with respect to kyanite + corundum. Table 2 shows that the solubility overestimation can be drastically lowered if an appropriate amount of silica is already dissolved in the starting fluid (Fig. 3). Experimentally, this can be achieved by introducing a definite amount of quartz in the external tube. Newton & Manning (2002) were the first to add quartz in the external tube of their setup with the aim of approaching equilibrium from silica-supersaturated conditions, with respect to the mineral assemblage enstatite + forsterite. Furthermore, they observed that the addition of quartz in the external tube reduces the dispersion of apparent solubility values obtained by the weight-loss technique,

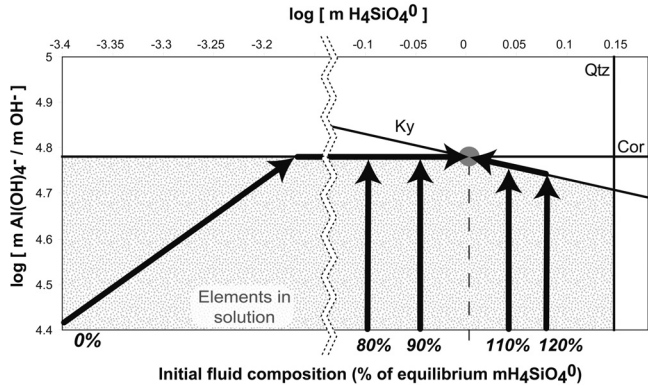

Fig. 3. Molality diagram, log ([m $Al(OH)_4^-$] / [m OH^-]) *vs.* log [m $H_4SiO_4^0$], showing the fluid saturation curves with respect to corundum (Cor), kyanite (Ky) and quartz (Qtz) at 800 °C – 1.2 GPa. These curves limit the field of fluid undersaturation with respect to all minerals considered (shaded area). The bold lines with black arrows underline the partial equilibrium reaction paths of the fluid while it equilibrates with the starting minerals kyanite + corundum (molar ratio of 1/1). The initial minerals are considered to produce two dominant aqueous species: $Al(OH)_4^-$ and $H_4SiO_4^0$. Solubility data were taken from Newton & Manning (2003). Each arrow represents a different composition of the initial fluid, determined by the amount of quartz placed in the external tube and expressed as a percentage of the equilibrium aqueous-Si molality. The dashed line represents the equilibrium molality of aqueous-Si (m_{Si}) *i.e.*, 100% On both sides of this line, the apperent m_{Si} derived from weight-loss measurements in a tube-in-tube setup, increases as a function of the initial fluid composition. The maximum overestimation of m_{Si} (*i.e.*, considering all the secondary phases in the external tube) for each of these initial fluid compositions is reported in Table 2.

even when it leads to a fluid which is undersaturated in silica with respect to that mineral assemblage at HT and HP. This experimental fact can be understood in the frame of fluid reaction paths. The presence of dissolved silica in the starting fluid limits secondary phase crystallization along the fluid reaction path (Fig. 3). In turn, the derived solubility data are better constrained (Table 2).

However, controlling the saturation state of the initial fluid in the external tube is not straightforward. It requires that the quartz dissolution is much faster than the dissolution of the mineral assemblage in the inner capsule. This may be achieved by using very fine-grained quartz powder in the external tube and large single crystal(s) of starting mineral (or mineral assemblage) in the inner capsule. Amorphous silica may also be a good candidate for "instantaneous dissolution", when determining the solubility of mineral assemblages free of quartz.

It is important to note that, whatever the silica content of the starting fluid (*i.e.*, undersaturation or supersaturation in silica with respect to the mineral assemblage of interest), secondary phases are expected to form as the result of incongruent dissolution or recrystallization, respectively. These secondary phases may partly crystallize in the external tube, leading in both cases to an overestimation of the aqueous-Si molality measured by the quench techniques. Thus, approaching the solubility by both under- and

Table 2. Maximum overestimate of the apparent aqueous-Si molality (m_{Si}) in equilibrium with the assemblage corundum + kyanite (molar ratio 1/1) using the weight-loss technique, for various silica content of the initial fluid, at 800 °C – 1.2 GPa.

Initial fluid composition (% m_{Si}) [a]	0 %	80 %	90 %	95 %	110 %	120 %
Maximum overestimation of m_{Si} [b]	170 %	34 %	17 %	9 %	27 %	54 %

[a] Determined from the amount of quartz placed in the external tube (assuming its instantaneous dissolution) and expressed in percentage of the equilibrium aqueous-Si molality.
[b] Calculated considering that all the secondary phases, due to incongruent dissolution of kyanite + corundum, occurred in the external tube of the tube-in-tube setup. Calculations assume a partial equilibrium fluid reaction path. Solubility data are taken from Newton & Manning (2003).

super-saturation sides actually does not bracket the mineral solubility. However, the true solubility of the mineral assemblage at a given P and T can be approached by successive experiments in which the amount of quartz in the external tube (*i.e.*, the silica molality of the initial fluid) is each time increased. For the case of corundum + kyanite at 800 °C – 1.2 GPa (data from Newton & Manning, 2003), Fig. 3 depicts a series of partial equilibrium fluid reaction paths resulting from different amounts of quartz in the external tube (assuming its instantaneous dissolution). Assumptions and equations are similar to those considered above. For each of these reaction paths, Table 2 gives the maximum overestimation (*i.e.*, considering all secondary phases in the external tube) of the apparent aqueous-Si molality derived from weight-loss measurements in a tube-in-tube setup. As the starting composition of the fluid approaches the equilibrium $H_4SiO_4^0$ concentration at 800 °C – 1.2 GPa, the apparent solubility of the mineral assemblage decreases towards its true solubility value (Table 2, Fig. 3). Subsequent addition of quartz in the initial fluid will cause silica supersaturation with respect to the mineral assemblage, and will thus result in an increase of the apparent solubility. Therefore, the true solubility of the mineral assemblage cannot be bracketed but only approached with this experimental procedure. The derived solubility will be overestimated in most cases or, at best, correct.

Potentially, the addition of silica to the external tube is a way to better constrain the solubility measurement using the tube-in-tube setup. The derived solubility data provides an upper bound to the true solubility of the considered solid(s). This true solubility can be attained if the optimal silica concentration in the external tube is found. However, this iterative approach is time-consuming and requires a constant setup geometry to be reproducible.

Acknowledgements: We thank Christian Chopin for careful reading and constructive comments of an early version of the manuscript. William M. Murphy and Bruno Goffé are acknowledged for fruitful discussions and their input in this project. Thanks are due to Michael Burchard and an anonymous reviewer for their careful and constructive reviews. Dominique Lattard (associate editor) is acknowledged for numerous constructive comments that greatly helped at improving the manuscript. This work was funded by DyETI (INSU-CNRS 2004-2005) and ECODEV (EC 6th PRTD 2002-2006).

References

Anderson, G.M. & Burnham, C.W. (1965): Solubility of quartz in supercritical water. *Am. J. Sci.*, **263**, 494-511.

—, — (1967): Reactions of quartz and corundum with aqueous chloride and hydroxide solutions at high temperatures and pressures. *Am. J. Sci.*, **265**, 12-27.

—, — (1983): Feldspar solubility and the transport of aluminum under metamorphic conditions. *Am. J. Sci.*, **283A**, 283-297.

Anderson, G.M., Pascal, M.L., Rao, J.G. (1987): Aluminum speciation in metamorphic fluids. *in* "Chemical transport in metasomatic processes", H.C. Helgeson, ed., D. Reidel Publ. Co., 927-321.

Azaroual, M., Pascal, M.L., Roux, J. (1996): Corundum solubility and aluminum speciation in KOH aqueous solutions at 400 °C from 0.5 to 2.0 kbar. *Geochim. Cosmochim. Acta*, **60**, 4601-4614.

Gunter, W.D. & Eugster, H.P. (1980): Mica-feldspar equilibria in supercritical alkali chloride solutions. *Contrib. Mineral. Petrol.*, **75**, 235-250.

Helgeson, H.C. (1968): Evaluation of irreversible reactions in geochemical processes involving minerals and aqueous solutions. I. Thermodynamic relations. *Geochim. Cosmochim. Acta*, **32**, 853-877.

— (1979): Transfer among minerals and hydrothermal solutions. *in* "Geochemistry of hydrothermal ore deposits", H.L. Barnes, ed., John Wiley and Sons, New York, 568-606.

Helgeson, H.C., Brown, T.H., Nigrini, A., Jones, T.A. (1970): Calculation of mass transfer in geochemical processes involving aqueous solutions. *Geochim. Cosmochim. Acta*, **34**, 569-592.

Johnson, J.W., Oelkers, E.H., Helgeson, H.C. (1992): SUPCRT92: a software package for calculating the standard molal thermodynamic properties of minerals, gases, aqueous species, and reactions from 1 to 5000 bar and 0 to 1000 °C. *Computers & Geosciences*, **18**, 899-947.

Manning, C.E. (1994): The solubility of quartz in H_2O in the lower crust and upper mantle. *Geochim. Cosmochim. Acta*, **58**, 4831-4839.

Manning, C.E. & Boettcher, S.L. (1994): Rapid-quench hydrothermal experiments at mantle pressures and temperatures. *Am. Mineral.*, **79**, 1153-1158.

Newton, R.C. & Manning, C.E. (2002): Solubility of enstatite plus forsterite in H_2O at deep crust/upper mantle conditions: 4 to 15 kbar and 700 to 900 °C. *Geochim. Cosmochim. Acta*, **66**, 4165-4176.

Newton, R.C. & Manning, C.E. (2003): Activity coefficient and polymerization of aqueous silica at 800 °C, 12 kbar, from sol-

ubility measurements on SiO_2-buffering mineral assemblages. *Contrib. Mineral. Petrol.*, **146**, 135-143.

Pascal, M.L. (1984): Nature et propriétés des espèces en solution dans le système K_2O-Na_2O-SiO_2-Al_2O_3-H_2O-HCl: contribution expérimentale. Thèse de Doctorat d'Etat, Université Pierre et Marie Curie, Paris.

Pascal, M.L. & Anderson, G.M. (1989): Speciation of Al, Si, and K in supercritical solutions: experimental study and interpretation. *Geochim. Cosmochim. Acta*, **53**, 1843-1855.

Pokrovski, G.S., Schott, J., Hazemann, J.L., Farges, F., Pokrovsky, O.S. (2002a): An X-ray absorption fine structure and nuclear magnetic resonance spectroscopy study of gallium-silica complexes in aqueous solution. *Geochim. Cosmochim. Acta*, **66**, 4203-4222.

Pokrovski, G.S., Zakirov, I.V., Roux, J., Testemale, D., Hazemann, J.L., Bychkov, A.Y., Golikova, G.V. (2002b): Experimental study of arsenic speciation in vapor phase to 500 °C: Implications for As transport and fractionation in low-density crustal fluids and volcanic gases. *Geochim. Cosmochim. Acta*, **66**, 3453-3480.

Pokrovski, G.S., Schott, J., Garges, F., Hazemann, J.L. (2003): Iron (III)-silica interactions in aqueous solution: Insights from X-ray absorption fine structure spectroscopy. *Geochim. Cosmochim. Acta*, **67**, 3559-3573.

Pokrovskii, V.A. & Helgeson, H.C. (1991): Unified description of incongruent reactions and mineral solubilities as a function of bulk composition and solution pH in hydrothermal systems. *Can. Mineral.*, **29**, 909-942.

Sanchez-Valle, C., Martinez, I., Daniel, I., Philippot, P., Bohic, S., Simionovici, A. (2003): Dissolution of strontianite at high P-T conditions: An *in-situ* synchrotron X-ray fluorescence study. *Am. Mineral.*, **88**, 978-985.

Sanchez-Valle, C., Daniel, I., Martinez, I., Simionovici, A., Reynard, B. (2004): Progress in quantitative elemental analyses in high P-T fluids using synchrotron x-ray fluorescence (SXRF). *J. Phys. Condens. Matter*, **16**, S1197-S1206.

Schmidt, C. & Rickers, K. (2003): *In-situ* determination of mineral solubilities in fluids using a hydrothermal diamond-anvil cell and SR-XRF: Solubility of AgCl in water. *Am. Mineral.*, **88**, 288-292.

Shock, E.L., Sassani, D.C., Willis, M., Sverjensky, D.A. (1997): Inorganic species in geologic fluids: Correlations among standard molal thermodynamic properties of aqueous ions and hydroxide complexes. *Geochim. Cosmochim. Acta*, **61**, 907-950.

Verlaguet, A., Brunet, F., Goffe, B., Murphy, W.M. (2006): Experimental study and modelling of fluid reaction paths in the quartz-kyanite +/– muscovite-water system at 0.7 GPa in the 350-550 °C range: Implications for Al selective transfer during metamorphism. *Geochim. Cosmochim. Acta*, **70**, 1772-1788.

Walther, J.V. & Orville, P.M. (1983): The extraction quench technique for determination of the thermodynamic properties of solute complexes - Application to quartz solubility in fluid mixtures. *Am. Mineral.*, **68**, 731-741.

Woodland, A.B. & Walther, J.V. (1987): Experimental determination of the solubility of the assemblage paragonite, albite, and quartz in supercritical H_2O. *Geochim. Cosmochim. Acta*, **51**, 365-372.

Zhang, Y.G. & Frantz, J.D. (2000): Enstatite-forsterite-water equilibria at elevated temperatures and pressures. *Am. Mineral.*, **85**, 918-925.

Zotov, N. & Keppler, H. (2000): *In-situ* Raman spectra of dissolved silica species in aqueous fluids to 900 °C and 14 kbar. *Am. Mineral.*, **85**, 600-603.

—, — (2002): Silica speciation in aqueous fluids at high pressures and high temperatures. *Chem. Geol.*, **184**, 71-82.

Received 20 December 2006
Modified version received 23 July 2007
Accepted 30 July 2007